



The effect of fluorine ion on fabrication of nanostructure forsterite during mechanochemical synthesis

M.H. Fathi*, M. Kharaziha

Department of Materials Engineering, Isfahan University of Technology, Isfahan 84156-83111, Iran

ARTICLE INFO

Article history:

Received 15 April 2008

Received in revised form 5 May 2008

Accepted 6 May 2008

Available online 24 June 2008

Keywords:

Ceramics

Mechanochemical processing

Nanostructure materials

ABSTRACT

Pure nanocrystalline forsterite could be fabricated by mechanochemical synthesis in the presence of fluorine ion. Mechanochemical process and post-heat treatment were performed using MgCO_3 , SiO_2 and $(\text{NH}_4)_2\text{SiF}_6$ powders as starting materials. Thermogravimetric analysis (TGA), Fourier transform infrared spectroscopy (FT-IR), X-ray diffraction (XRD) and scanning electron microscopy (SEM) techniques were utilized to characterize the synthesized powders. Pure forsterite could be obtained after 5 h of mechanical activation and post-heat treatment for 1 h at 900°C . Nanocrystalline forsterite was fabricated with the grain size of about 30 nm. The synthesized forsterite nanopowder had particle size smaller than 100 nm. The results showed that in the presence of fluorine ion, the rate of forsterite formation was increased by combustion reaction.

© 2008 Elsevier B.V. All rights reserved.

1. Introduction

Mechanical activation (MA) has been widely used to synthesize a variety of materials such as nanocrystalline materials [1], intermetallic compounds [2], and composites [3,4]. In almost all cases, the final product has nanosize structure which exhibits better properties and performance in comparison to the conventional coarse-grain materials [5]. Chemical reactions induced by mechanical treatment, i.e. mechanochemical synthesis, are known to be very effective for preparing nanocrystalline powders consisting of more than two phases [6].

Forsterite (Mg_2SiO_4) is a crystalline magnesium silicate ceramic which belongs to the group of olivine [7]. Forsterite is an ideal substrate material for electronics and suitable material for engineers and designers, especially as an active medium for tunable laser [8,9].

Nanocrystalline materials can possess good biocompatibility and might be suitable for biomedical application [10]. Recent investigations suggest that forsterite ceramics possess good biocompatibility and mechanical properties and might be suitable for potential application, like bone implant materials [11].

Since the reaction of silicate formation starting with appropriate oxides is generally sluggish due to the relatively low diffusivity of formed compounds, pure forsterite cannot be fabricated and enstatite (MgSiO_3) may be formed. It is very difficult to

avoid the formation of MgSiO_3 and/or MgO , and thermal treatments up to $1200\text{--}1600^\circ\text{C}$ are necessary to obtain pure forsterite [12].

The presence of enstatite (MgSiO_3) in forsterite refractories can be detrimental to the high temperature properties and behavior because enstatite dissociates into forsterite and a SiO_2 -rich liquid at 1557°C [13]. This matter causes difficulty during the sintering of forsterite at high temperatures. Enstatite ceramics possess good mechanical properties but there are four different polymorphs of enstatite which are unstable and may affect mechanical properties. The changes from one form to another depend on temperature, pressure, internal stress in grains and grain size, etc. So, the parameters of the fabrication process should be strictly controlled [14,15]. In comparison to enstatite, results show that the mechanical strength of forsterite is similar to that of enstatite. In addition, no detrimental phase transformations occur during processing of forsterite [10].

Several methods have been employed to prepare pure forsterite; including heating MgO and SiO_2 powders (the reaction temperature is up to 1525°C) [16], co-precipitation [17] and sol-gel techniques [18–21].

Burlitch et al. [22] succeeded in preventing the phase separation of MgO in an all alkoxides sol-gel process by hydrolyzing the alkoxides with hydrogen peroxide. The crystallization occurred at 750°C and fully crystallized single-phase forsterite was obtained at 1000°C . Saberi and Alinejad synthesized [23] nanocrystalline forsterite by a polymer matrix method. Crystallite size of prepared forsterite was in the range of $10\text{--}30\text{ nm}$ and, its particle size was smaller than 200 nm in the calcined sample at 800°C .

* Corresponding author. Tel.: +98 311 3915708; fax: +98 311 3912752.

E-mail addresses: fathimoh@yahoo.com, fathi@cc.iut.ac.ir (M.H. Fathi).

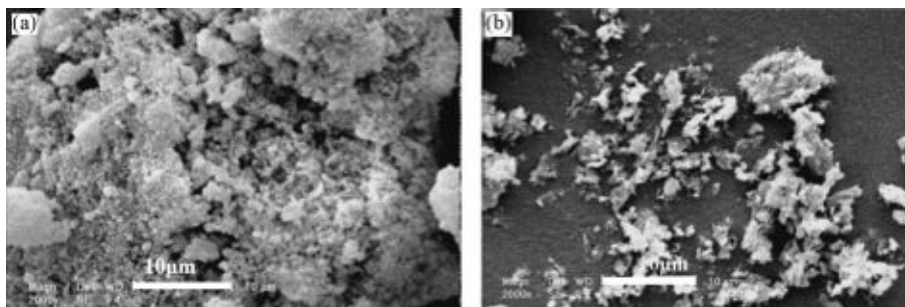


Fig. 1. SEM micrograph of starting materials including: (a) SiO₂ and (b) MgCO₃ powders.

Fabrication of forsterite by MA method has been investigated by researchers but preparation of pure forsterite has not been reported [24,25]. They reported that forsterite could be obtained by MA and heat treatment at 1200 °C, but finally the amount of enstatite could be recognized and pure forsterite could not be fabricated [24]. Kosanovi [25] also reported that forsterite could be obtained by ball milling and 3 h of heat treatment at 1000 °C. In this method, no reaction occurred during milling between template materials after 10 h of milling.

The objective of this work was to synthesize pure nanocrystalline forsterite powder by mechanical activation and post-heat treatment method, and to evaluate the effect of fluorine ion presence on the reactions rate.

2. Experimental

2.1. Powder preparation

The starting materials were high-purity MgCO₃ (Riedel-de Haen 99.9%) and amorphous SiO₂ (Aldrich Chemical Company, 99.9%). Amorphous SiO₂ was selected to increase the rate of reactions [26]. Fig. 1 shows the morphology of starting materials powders. The SiO₂ particles had an irregular shape with a size distribution of 6–40 µm. MgCO₃ particles were nearly uniform in size (10 µm) with an irregular morphology. The procedure of forsterite preparation consisted of two steps; high-energy mechanical activation (ball milling) and post-heat treatment. The starting materials powders with stoichiometric composition of forsterite (sample-A) were weighed, mixed, and ball-milled with planetary ball milling for various periods of time using zircon as the grinding media (ball and cup). The weight of ball to powder ratio was selected 25:1 and the time of milling was selected 10 min, and 1, 5, 10 and 15 h. For estimating the effect of fluorine ion (NH₄)₂SiF₆ (Aldrich Chemical Company, 99.9%), powder was added to sample-A (namely, sample-B). The powders of MgCO₃:SiO₂:(NH₄)₂SiF₆ with stoichiometric composition of forsterite were weighed with molar ratios 2:0.85:0.15. After milling, the obtained powders were heat treated for 1 h at different temperatures in air atmosphere and isothermal condition at 700–1200 °C.

2.2. Powder characterization

The crystallographic structural analysis was carried out by X-ray diffraction (XRD) method using a Philips X'Pert MPD diffractometer (Cu K α radiation: $\lambda = 0.154056$ nm at 40 kV and 30 mA) over the 2θ range of 20–80° at a scan rate of 0.05°/min. The morphology and particle size of the milled powders were analyzed by scanning electron microscopy (SEM) using a Philips XL30. Weight losses on heating were measured using thermogravimetric analysis (TGA) at the temperature ranging from room temperature to 1200 °C in air at heating rate of 10 °C/min. Fourier transform infrared (FT-IR) spectroscopy analysis (Bomem, MB 100) was carried out to identify the functional groups. The spectrum was recorded in the 4000–400 cm⁻¹ region with 2 cm⁻¹ resolution. The apparent crystallite sizes of the powders were determined using the Williamson–Hall's equation [27]:

$$\beta \cos \theta = \frac{0.9\lambda}{t} + \varepsilon \cos \theta \quad (1)$$

where t is the grain size, λ the wavelength ($\lambda = 0.154056$ nm), β the width of peak in the middle of its height, θ the Bragg's angle and ε is the residual strain in powder.

3. Results and discussion

3.1. Thermal analysis

TGA and DTG curves of sample-A powder, after mechanical activation for 10 h, are shown in Fig. 2. Weight losses occurred in three main stages. The first stage occurred below 340 °C probably due to loss of water through hydration. The second stage occurred below 500 °C due to decomposition of the magnesium carbonate and crystallization of MgO, and the third stage occurred below 820 °C due to the crystallization of forsterite. No further significant weight loss could be observed above 820 °C.

TGA curves of sample-B powders which were mechanically activated for 5 and 10 h are shown in Fig. 3. The weight losses of 5 and 10 h mechanically activated samples up to 38% and 31% could be recognized, respectively. During the heating of sample-B powder which was mechanically activated for 5 h, a weight loss (about 18%) due to adsorbed and structural water could be observed below 200 °C. Larger weight loss (about 25%) occurred below 400 °C, ascribable to loss of organic substances and fluorine ion. The next stage, between 400 and 600 °C, could be ascribed to the removal of residual carbon from pores and the final stage could be ascribed to the crystallization of forsterite. Part (b) of Fig. 3 shows the DTG curve of sample-B powder after 5 h of mechanical activation. The curve shows a peak around 806 °C which indicates the formation of forsterite.

It can be seen in part (a) of Fig. 3 that after 10 h mechanical activation, weight losses occurred in three main stages. The first stage (about 10% weight loss) occurred below 200 °C and is probably caused by removal of structural water. The second stage, between 200 and 300 °C (about 30% weight loss), could be ascribed to the removal of residual organic groups and fluorine ion to form HF. Removal of residual carbon from pores was a slow process, and contributes to the third stage. This continues to around 1000 °C above which no further loss could be observed indicating that forsterite formation could occur during mechanical activation.

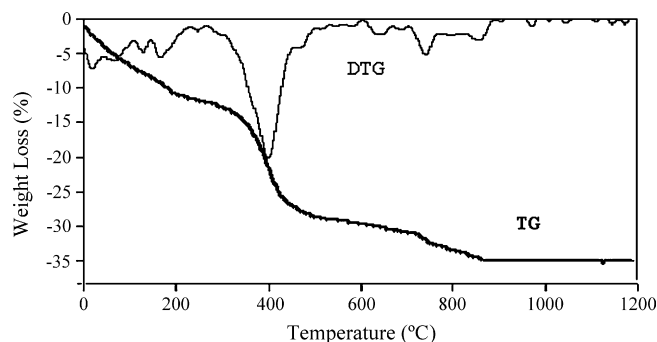


Fig. 2. TGA and DTG curves of sample-A powder after 10-h mechanical activation.

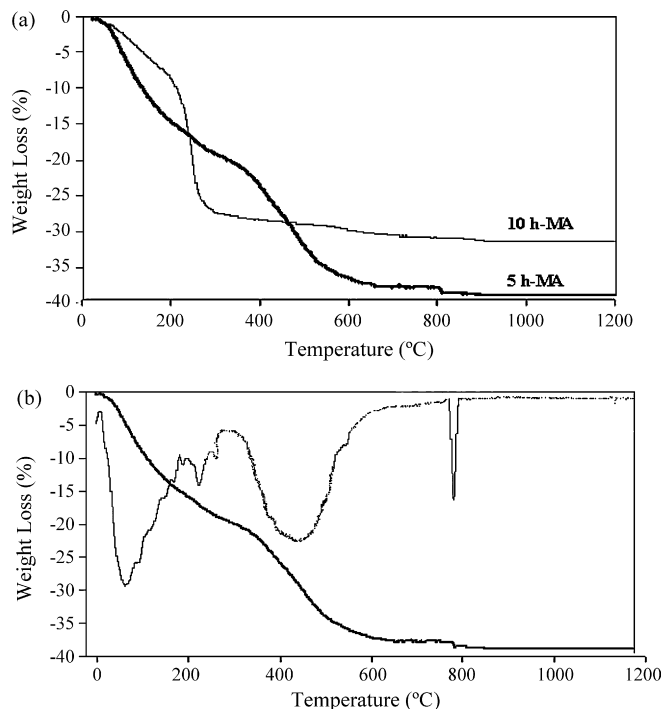
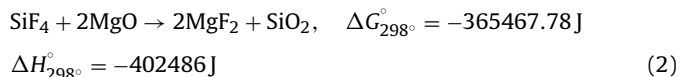


Fig. 3. (a) TGA curves of sample-B powders after 5 and 10-h mechanical activation and (b) TGA and DTG curves of sample-B powder after 5-h mechanical activation.

3.2. Phase evolution and reaction mechanism

X-ray diffraction patterns of sample-B powders which were mechanically activated for 10 min, and 1, 5, 10, and 15 h are given in Fig. 4. It can be seen that the starting materials of MgCO_3 and $(\text{NH}_4)_2\text{SiF}_6$ could remain after 10 min of mechanical activation (MA). After 1 h MA, the peaks of XRD patterns of starting materials disappeared and MgO and MgF_2 phases could be detected indicating the occurrence of the combustion reaction. On the basis of reported analysis [24], the chemisorption of SiF_4 which was fabricated by decomposition of $(\text{NH}_4)_2\text{SiF}_6$, on the MgO base particles could be accepted. In this condition, MgF_2 could be synthesized by mechanochemical reaction during ball milling of a stoichiometric mixture of MgO and SiF_4 [28] according to the reaction of the following equation:



During mechanical activation at room temperature, SiF_4 - MgO reaction (Eq. (2)) could thermodynamically occur due to its negative

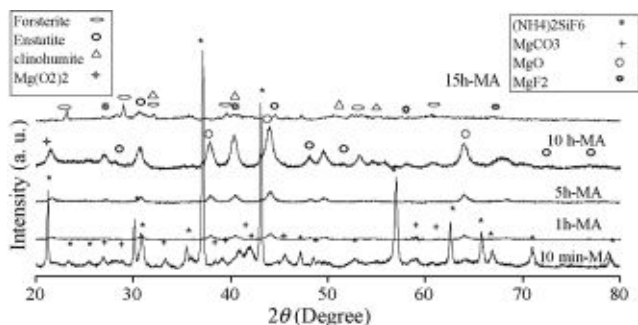


Fig. 4. XRD patterns of sample-B powder after mechanical activation for different periods of time.

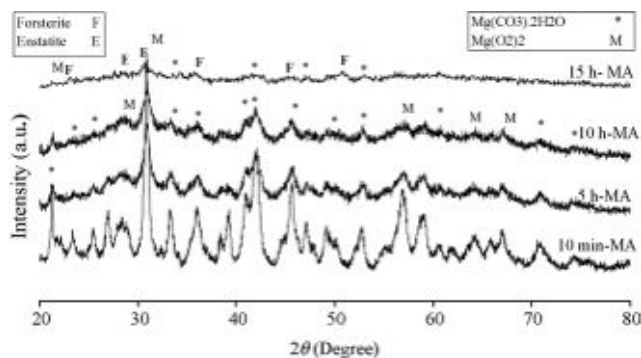


Fig. 5. XRD patterns of sample-A powder after mechanical activation for various periods of time.

free energy change. ΔH_{298}° for SiF_4 - MgO reaction is also negative indicating that reaction of Eq. (2) is highly exothermic and leads to an increase in the vial temperature. The adiabatic temperature, T_{ad} , for Eq. (2) is 1747°C . It has been reported that the value of adiabatic temperature T_{ad} should be above 1527°C in thermally ignited systems [29]. It was therefore expected that a combustion reaction take place during mechanical activation of powder mixture.

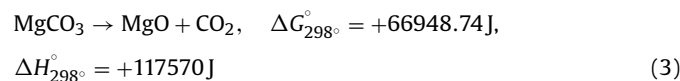
After 1 h of mechanical activation, MgO peaks could be observed. Obtained heat of the reaction of Eq. (2) caused decomposition of MgCO_3 to MgO . The reasons of the decomposition can be explained in this manner:

- (1) The decomposition of compounds during mechanical activation was enhanced in the presence of another compound with which the reaction product can react. Reaction between MgO and SiF_4 caused the decomposition of MgCO_3 .
- (2) Increasing the temperature as the result of combustion reaction (Eq. (2)).

By increasing the time of milling up to 10 h, no composition changes of the powder could be obtained, but the crystallinity of starting materials reduced. TG curves show that forsterite could be fabricated during mechanical activation. Thus, forsterite must be amorphous after 10 h of mechanical activation. By increasing the time of milling up to 15 h, the crystallinity of powder reduced and new compositions such as $(\text{Mg}_2\text{SiO}_4)_4$ - $\text{Mg}(\text{F}, \text{OH})_2$ (clinohumite), MgSiO_3 (enstatite) and partial forsterite could be fabricated. Clinohumite is a compound of the humite groups which could be fabricated during mechanical activation process.

X-ray pattern of sample-A powder, which was mechanically activated for 10 min, 5, 10 and 15 h, are shown in Fig. 5. The result shows that decomposition of MgCO_3 during mechanical activation is very slow and MgCO_3 could be stable after 10 h of MA.

Eq. (3) shows decomposition of MgCO_3 . Decomposition of MgCO_3 has positive free energy change and ΔH_{298}° of the decomposition reaction is also positive indicating that reaction is endothermic (Eq. (3)). Thus, decomposition of MgCO_3 is very slow and could not be done at initial times of mechanical activation.



Forsterite can be synthesized by reaction of a stoichiometric mixture of MgO and SiO_2 according to the following:



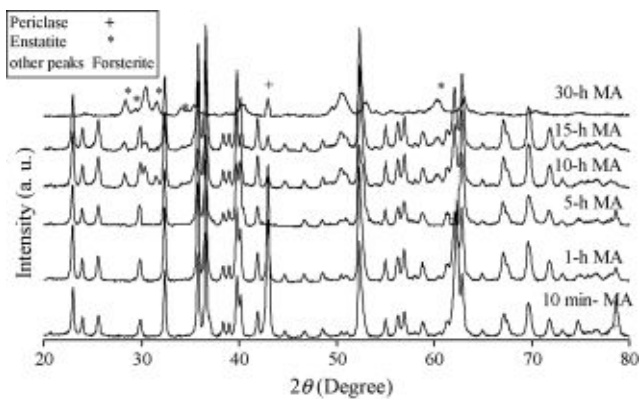


Fig. 6. XRD patterns of sample-B powder after mechanical activation for various periods of time and heat treatment for 1 h at 1000 °C.

SiO₂–MgO reaction can thermodynamically occur due to its negative free energy change (Eq. (4)). ΔH_{298}° for SiO₂–MgO reaction is also negative indicating that the reaction is exothermic, but the adiabatic temperature, T_{ad} , for this reaction is 454 °C. Thus, formation of forsterite could be performed by a diffusion-controlled mechanism. Brindley and Hayami reported that MgO initially diffuses into the surface of the SiO₂ to form enstatite and diffusion continues through this enstatite layer to form forsterite [18].

In order to eliminate fluorine ion from the compound, heat treatment must be performed after mechanical activation. Obtained results indicated that the loss of fluorine during heat treatment while the system is open to air and the water vapor from surrounding becomes an active reactant and allows the slow hydrolysis of MgF₂ or clinohumite from humite group compounds.

In order to determine the effect of mechanical activation process on forsterite fabrication, heat treatment was performed at 1000 °C. X-ray diffraction patterns of sample-B powders which were mechanically activated for 10 min, 1, 5, 10, 15, 30 h, and were heat treated at 1000 °C are given in Fig. 6. It could be seen that by 10 min mechanical activation, the crystalline forsterite was formed but the main phase of prepared powder would be MgO. After 1 h of mechanical activation and heat treatment at 1000 °C, forsterite could be fabricated but MgO could also be recognized. When mechanical activation was done for 5 h, forsterite could be completely fabricated. By increasing the time of mechanical activation up to 15 h, besides forsterite, the trace of enstatite (MgSiO₃) and periclase (MgO) could be recognized. Even by increasing the

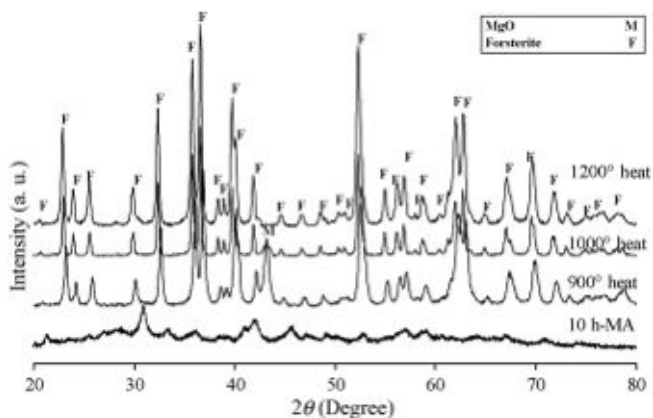


Fig. 7. XRD patterns of sample-A powder after 10-h mechanical activation and 1-h heat treatment at various temperatures.

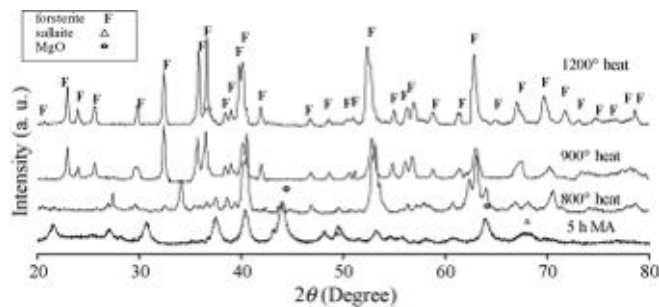


Fig. 8. XRD patterns of sample-B powder after 5-h mechanical activation and 1-h heat treatment at various temperatures.

Table 1
d-Spacing of the prepared powder in comparison with the JCPDC card

d (nm)	Intensity		hkl	
	JCPDC	Experimental		
JCPDC	Experimental	JCPDC	Experimental	JCPDC
3.8819	3.8812	75.8	76	120
3.4895	3.4990	30	26	111
2.7651	2.7653	65.6	66	031
2.5095	2.5097	86	83	131
2.4548	2.4566	100	100	211
2.2467	2.2473	37	37	041
1.7478	1.7482	67	73	222
1.4957	1.4954	30	31	400
1.4782	1.4780	33	33	260

time of mechanical activation up to 30 h, enstatite and periclase would not be eliminated and could be stable.

Appearance of CO₂ during mechanical activation from decomposition of magnesium carbonate might be the cause of the enstatite and MgO fabrication during mechanical activation and stabilization of these phases until high temperatures. Previous studying shows that in the Mg₂SiO₄–CO₂ system, even with a minute amount of CO₂, not only Mg₂SiO₄ but also MgSiO₃ and SiO₂ are present [30].

During the process of forsterite synthesis, it is important to control the phase development. Even by heating at 1540 °C for 5 h, that is a temperature close to the melting point of enstatite, MgSiO₃ and MgO would not completely react together to form Mg₂SiO₄ [12]. This situation is frequently encountered during the synthesis of forsterite. Increasing the time of mechanical activation causes enstatite formation. In this condition, enstatite is stable up to high temperature. Kazakos et al. [20] noted that heat treatment did not have any obvious effect on the enstatite phase until a firing temperature near 1600 °C was reached.

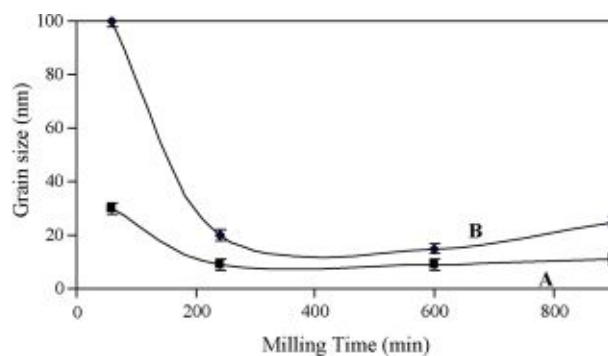


Fig. 9. Crystallite sizes of two main groups of samples (sample-A and sample-B) as a function of the time of mechanical activation.

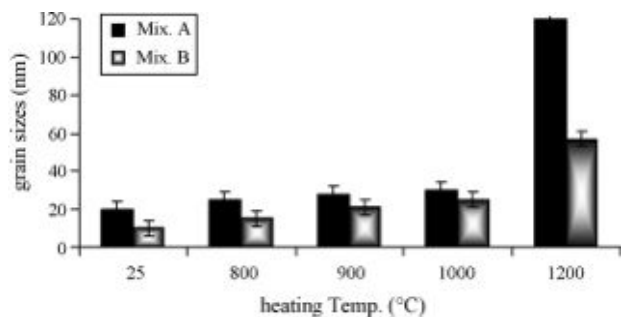


Fig. 10. Crystallite sizes of two main groups of sample (A and B) after 10 and 5-h mechanical activation and heat treatment at different temperatures.

Fig. 7 shows the effect of 1-h heat treatment at various temperatures on the sample-A powders which were mechanically activated for 10 h. In this condition, the forsterite (Mg_2SiO_4) and periclase (MgO) could be fabricated. After heating to 1000°C , the powder exhibits a better crystallinity but MgO is still present indicating that for obtaining the global stoichiometry 2:1 for $\text{Mg}:\text{Si}$ in forsterite, some amorphous silica or indiscernible MgSiO_3 should remain in the sample. After heating at 1200°C for 1 h, the MgSiO_3 or amorphous silica reacted with MgO , and Mg_2SiO_4 appeared as a single phase.

The XRD patterns of sample-B powder after 5 h of mechanical activation and heat treatment at 800 , 900 and 1200°C for 1 h are shown in Fig. 8. After heating to 800°C , the crystallization of forsterite was evident but the other peaks such as MgO and MgF_2 could also be recognized. After heating to 900°C , the powder exhibited complete formation of forsterite.

The result shows that after 1 h heating at 1200°C , forsterite was stable and did not decompose to the other composition such as enstatite (MgSiO_3). Therefore, forsterite could be completely fabricated by 5 h of mechanical activation and 1 h heat treatment at 900°C . Detailed analysis of the changes of the MgO diffraction line intensities, as one of the possible parameters for describing the reaction advance, showed that the fluorine ion caused an increase in the reaction rates.

Fluorine ion caused decomposition of magnesium carbonate to magnesium oxide only after 1 h of mechanical activation. Increasing the temperature obtained from the combustion reaction (Eq. (2)) was not enough to fabricate forsterite but by increasing the time of mechanical activation up to 10 h, forsterite could be fabricated. Also, pure forsterite could be fabricated by only 5 h of mechanical activation and 1 h of heat treatment at 900°C in the presence of fluorine ion. Mechanical activation of the mixture basic MgCO_3 and amorphous SiO_2 , in the presence of $(\text{NH}_4)_2\text{SiF}_6$, affects the mechanism of forsterite formation via different compounds and increases the rate of reaction.

The d spacing of some of the (hkl) of the prepared forsterite powder are compared with the JCPDS [31] standard in Table 1. It can be seen that there is a good match with the standard both in terms of intensity and position of the peaks.

The crystallite size of obtained powder after mechanical activation and the crystallite size of forsterite, which was fabricated by 5 h of mechanical activation and heat treatment, could be determined. The crystallite size of the two main groups of sample-A and sample-B were calculated by using the peak width and is shown in Fig. 9.

An increase in grain size of sample-B powder was observed in comparison to sample-A powder. It could be due to the difference in formation mechanism. In sample-A powder, MgO was formed by diffusion phenomena at low temperature while in sample-B powder case, as mentioned before, MgO and MgF_2 were formed by a combustion manner at high temperature. By increasing the milling time, a dislocation cell structure is obtained which subsequently creates low-angle grain boundaries. With prolonged processing, this structure is transformed to fully nanocrystalline structure with completely random orientation of neighboring grains which are separated by high-angle grain boundaries. The grain size decreased continuously by increasing the milling time until a saturation size was approached. The grain size of sample-A powder was almost stable after 5 and up to 15 h of mechanical activation. The grain size of sample-B was reduced up to 10 h of mechanical activation and then increased. It is suggested that forsterite crystallization caused grain growth.

The crystallite sizes of the prepared forsterite of two main groups of samples are shown in Fig. 10 as a function of heating temperature. The forsterite crystallite size of 10 h of mechanically activated sample-A powder and 5 h of mechanically activated sample-B powder were calculated. In all different heating temperatures, the grain sizes of sample-B powder are larger than those of sample-A because of crystallite phases formation during mechanical activation which act as nuclei for the other phases which will be formed during next heat treatment.

3.3. SEM analysis

The SEM micrographs of sample-B powder particles after 5 h of mechanical activation before and after heat treatment at 900°C are shown in Fig. 11. As it can be seen, after 5 h of ball milling, particles have irregular shape with rather narrow size distribution. In fact, some parameters such as the size of particles produced during reactive milling, the attractive van der Waals forces and the tendency of the system to minimize the total surface or interfacial energy; and the low crystallinity of particles (amorphous structure) could affect the agglomeration of particles.

After heat treatment, the particles have more homogeneity distribution than before heat treatment and the particle sizes are less than 100 nm .

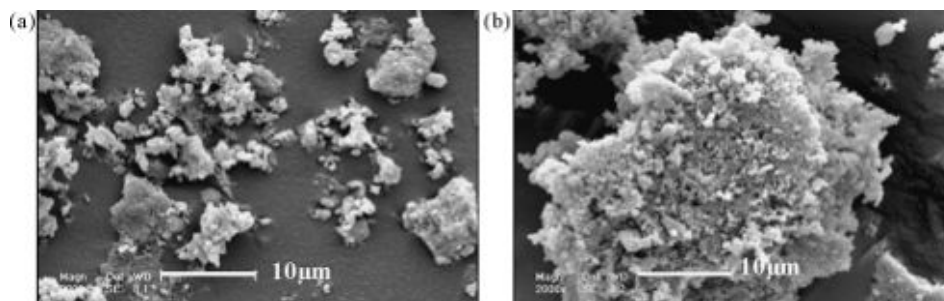


Fig. 11. SEM micrograph of 5-h mechanical activated sample-B powder: (a) before and (b) after heat treatment at 900°C .

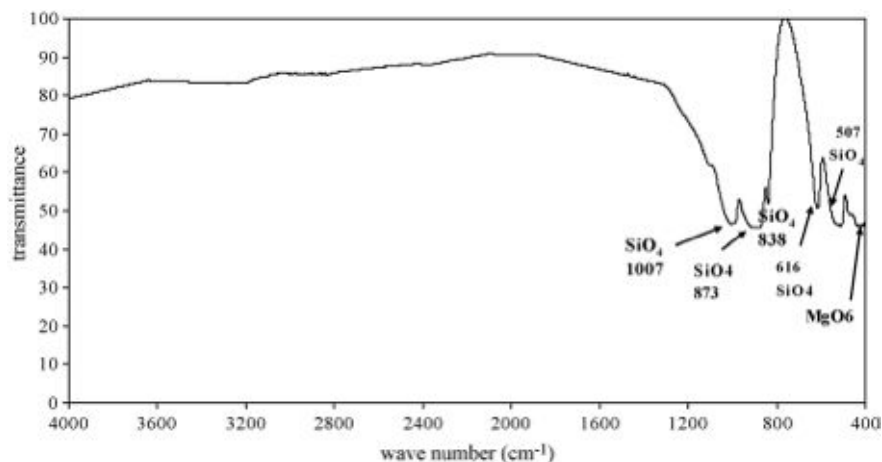


Fig. 12. The FT-IR spectra of prepared forsterite nanopowder which was heat treated at 900 °C.

3.4. FT-IR analysis

Fig. 12 illustrates FT-IR spectra of heat treated forsterite powder at 900 °C. FT-IR analysis shows peaks of Si–O bands in the SiO₄ tetrahedron that prove the formation of forsterite as it is shown in XRD pattern of this sample. The bands related to the characteristic peaks of forsterite appear in the range of 830–1000 cm⁻¹ (SiO₄ stretching), at 500–620 cm⁻¹ (SiO₄ bending) and at 475 cm⁻¹ for modes of octahedral MgO₆. Similar results were also reported in previous studies [32].

4. Conclusion

Pure nanocrystalline forsterite was successfully fabricated by 5 h of mechanical activation (MA) and heat treatment. MA besides fluorine ion enhances the forsterite formation in basic MgCO₃–amorphous SiO₂ mixture at lower temperature. (NH₄)₂SiF₆ can be decomposed during mechanical activation. SiF₄ is formed due to decomposition of (NH₄)₂SiF₆. The mechanochemical reaction between MgO and SiF₄ takes place in an explosive mode leading to the formation of MgO and MgF₂. In order to evacuate the fluorine ion, heat treatment must be performed. Fluorine ion can leave the powder by hydrolysis phenomena. Presence of (NH₄)₂SiF₆ causes formation of a series of compounds during mechanical activation that finally increase reaction rate and forsterite can be fully crystallized after 1 h of heat treatment at 900 °C. Without fluorine ion, forsterite can be fabricated by 10 h of mechanical activation and heat treatment at 1200 °C. Mechanical activation reduces the forsterite crystallite sizes up to about 30 nm and particle size smaller than 100 nm.

References

- [1] R. Hamzaoui, S. Guessasma, O. Elkedim, J. Alloys Compd. in press.
- [2] M. Krasnowski, A. Antolak, T. Kulik, J. Alloys Compd. 434 (2007) 344–347.
- [3] F. Li, L. Jiang, J. Du, S. Wang, J. Alloys Compd. 452 (2008) 421–424.
- [4] R. Maiti, M. Chakraborty, J. Alloys Compd. 458 (2008) 450–456.
- [5] G. Chen, G.X. Sun, Z.G. Zhu, Mater. Sci. Eng. A 265 (1999) 197.
- [6] L. Takacs, Prog. Mater. Sci. 47 (2002) 355–414.
- [7] C. Kosanovic, N. Stubicar, N. Tomasic, V. Bermanec, M. Stubicar, J. Alloys Compd. 389 (2005) 306–309.
- [8] I.T. Mckinnie, R.Y. Choie, Opt. Quant. Elect. 29 (1997) 605–610.
- [9] L. Lin, M. Yin, C. Shi, W. Zhang, J. Alloys Compd. 455 (2008) 327–330.
- [10] T.J. Webster, R.W. Siegel, R. Bizios, Biomaterials 21 (2002) 1803.
- [11] S. Ni, L. Chou, Ceram. Int. 33 (2007) 83–88.
- [12] A. DOUY, J. Sol–Gel Sci. Technol. 24 (2002) 221–228.
- [13] B.D. Matthew, J. Sol–Gel Sci. Technol. 15 (1999) 211–219.
- [14] W. Mielcarek, D. Nowak, K. Prociow, J. Eur. Ceram. Soc. 24 (2004) 3817–3821.
- [15] W.E. Lee, A.H. Heuer, J. Am. Ceram. Soc. 70 (1987) 349–360.
- [16] H.E. Swanson, E. Targe, Natl. Bur. Stand. (US) Circ. 359 (1953) 83–86.
- [17] O. Yamaguchi, Y. Nakajima, K. Shimazu, Chem. Lett. 401 (1976).
- [18] G.W. Brindley, R. Hayami, Phil. Mag. 12 (1965) 505.
- [19] P.S. Devi, H.D. Gafney, V. Petricevi, R.R. Alfano, J. Non-Cryst. Solids 203 (1996) 78.
- [20] A. Kazakos, S. Komarneni, R. Roy, Mater. Lett. 10 (1990) 405.
- [21] D.G. Park, J.C. Duchamp, T.M. Duncan, J.M. Burlitch, Chem. Mater. 6 (1994) 1990.
- [22] J.M. Burlitch, M.L. Beeman, B. Riley, Chem. Mater. 3 (1991) 692.
- [23] A. Saber, B. Alinejad, Mater. Res. Bull. 42 (2007) 666–673.
- [24] S.J. Kiss, E. Kostic, D. Djurovic, S. Boskovic, Powder Technol. 114 (2001) 84–88.
- [25] C. Kosanovi, N. Stubicar, N. Tomasic, V. Bermanec, J. Alloys Compd. 389 (2005) 306–309.
- [26] M.B. Thomas, R.H. Doremus, Am. Ceram. Soc. Bull. 60 (1981) 258–259.
- [27] K. Williamson, W.H. Hall, Acta Metall. 1 (1953) 22–31.
- [28] D.R. Gaskell, Introduction to Thermodynamics of Materials, third ed., Scripta Pub. Co., 1973.
- [29] Z.A. Munir, Am. Ceram. Soc. Bull. 67 (1988) 342.
- [30] L. Liu, Phys. Earth Planet. Int. 146 (2004) 261–272.
- [31] JCPDS Card no. 34-0189, 1984.
- [32] M.T. Tsai, J. Non-Cryst. Solids 298 (2002) 116–130.